

UC Irvine

UC Irvine Previously Published Works

Title

Phase Inhomogeneity of the Itinerant Ferromagnet MnSi at High Pressures

Permalink

<https://escholarship.org/uc/item/2q59d219>

Journal

Physical Review Letters, 92(8)

ISSN

0031-9007

Authors

Yu, W
Zamborszky, F
Thompson, JD
[et al.](#)

Publication Date

2004-02-27

DOI

10.1103/physrevlett.92.086403

Copyright Information

This work is made available under the terms of a Creative Commons Attribution License, available at <https://creativecommons.org/licenses/by/4.0/>

Peer reviewed

Phase Inhomogeneity of the Itinerant Ferromagnet MnSi at High Pressures

W. Yu¹, F. Zamborszky^{1,2}, J. D. Thompson², J. L. Sarrao², M. E. Torelli³, Z. Fisk³ and S. E. Brown¹

¹*Department of Physics and Astronomy, University of California at Los Angeles, Los Angeles, CA 90095-1547*

²*Los Alamos National Laboratory, Los Alamos, NM 87545 and*

³*National High Magnetic Field Laboratory, Florida State University, Tallahassee, FL 32310*

(Dated: December 21, 2013)

The pressure induced quantum phase transition of the weakly itinerant ferromagnet MnSi is studied using zero-field ²⁹Si NMR spectroscopy and relaxation. Below $P^* \approx 1.2\text{GPa}$, the intensity of the signal and the nuclear spin-lattice relaxation is independent of pressure, even though the amplitude of the magnetization drops by 20% from the ambient pressure amplitude. For $P > P^*$, the decreasing intensity within the experimentally detectable bandwidth signals the onset of an inhomogeneous phase that persists to the highest pressure measured, $P \geq 1.75\text{GPa}$, which is well beyond the known critical pressure $P_c = 1.46\text{GPa}$. Implications for the non-Fermi Liquid behavior observed for $P > P_c$ are discussed.

PACS numbers: 71.10.Hf, 75.50.Cc, 76.60.-k

In magnetically-ordered systems where the magnetism is weak, the possibility of tuning the transition temperature $T_c \rightarrow 0$ using an adjustable external parameter is of particular importance, because in the case that the transition is continuous, the Fermi Liquid description is expected to break down at the quantum critical point (QCP) [1]. Further, there are many systems known where the physical properties cannot be described as Fermi Liquids and so far, it is debated to what extent this can be accounted for by the proximity to a QCP. Recently, the ability to tune the magnetic ordering transition in ostensibly clean systems using high pressure was demonstrated for several itinerant ferromagnetic systems, including *MnSi* [2, 3], *ZrZn₂* [4], and *UGe₂* [5], as well as the antiferromagnet heavy-fermion systems *CeIn₃*, *CePd₂Si₂* [6], as well as several in the *CeMIn₅* family [7]. In many of these examples, non-Fermi Liquid behavior is observed over a range of temperatures and pressures, although applying theory to the experiments is not straight-forward for either case [8, 9].

Consider the weak itinerant ferromagnetism in MnSi, the most extensively studied of the weak ferromagnets. Its ambient-pressure properties are successfully described by the self-consistent renormalization (SCR) theory of spin fluctuations [10]. First, it is characterized by a Curie-Weiss (CW) form for the susceptibility, where the effective moments $\mu_{eff}(T > T_c)$ are much larger than the saturation moments $\mu_s(T \ll T_c)$ [11]. The low energy excitations probed by neutron scattering [12] and the critical behavior probed by NMR [13] and μSR [14] are consistent with exchange-enhanced spin fluctuations [10]. Below T_c , MnSi orders as a helimagnet with a very small wavevector, $Q \approx 2\pi(1, 1, 1)/180\text{\AA}$ [15], due to the Dzyaloshinski-Moriya (DM) interaction arising from spin-orbit coupling in the *B20* lattice structure lacking inversion symmetry [16]. The ground state is a Fermi Liquid [3]. With applied pressure, the transition temperature smoothly approaches zero temperature [2]. In ap-

proaching the critical pressure and beyond, there are several observations that fall outside the Hertz-Millis framework. First, at pressures starting from 1.2GPa and up to the critical pressure $P_c \approx 1.46\text{GPa}$, the transition is first order [3]. Next, it is known empirically that for a remarkably wide range of pressures $P > P_c$, the temperature-dependent part of the resistivity varies as $\Delta\rho \propto T^{3/2}$ to temperatures well below where the crossover to Fermi Liquid behavior is expected [17]. It appears to be a general phenomenon, as similar behavior is reportedly observed for *ZrZn₂* and *Ni₃Al* [9]. In the specific case of MnSi, for $P > 1.2\text{GPa}$, the relationship of the broad maximum in ac susceptibility [3] in the vicinity of the critical pressure and the non-Fermi Liquid behavior is unclear. These observations led Pleiderer, *et al.* [9], to question whether the ground state in nearly ferromagnetic metals is a Fermi Liquid at all. In addressing this question, NMR and $\mu^+\text{SR}$ ought to be a valuable probe of the local physics.

In this Letter, zero-field ²⁹Si NMR spectroscopy and dynamics on powdered samples of MnSi are presented, with particular emphasis on pressures in the vicinity of P_c . Due to the homogeneous and isotropic hyperfine coupling constant $A_{hf} = 58.7\text{kOe}/\mu_B$ [18], the NMR resonance from ²⁹Si gives approximately the local moment, about $0.4\mu_B/\text{Mn}$ at ambient pressure [11]. In monitoring the low temperature pressure and paying particular attention to quantifying pressure inhomogeneities, we find the spin dynamics, as inferred from $(T_1T)^{-1}$, undergoes a discontinuous change when the pressure exceeds $P^* \approx 1.2 - 1.3\text{GPa}$. Coincident with the change in dynamics is a smooth decrease in signal intensity for $P > P^*$. We find that the signal persists to the highest pressure we were able to measure, $P \approx 1.75\text{GPa}$, far beyond the quoted critical pressure $P_c = 1.46\text{GPa}$ [3]. The observations are consistent with a change in the magnetic state for pressures exceeding P^* , where the system also becomes inhomogeneous. Perhaps the unusual

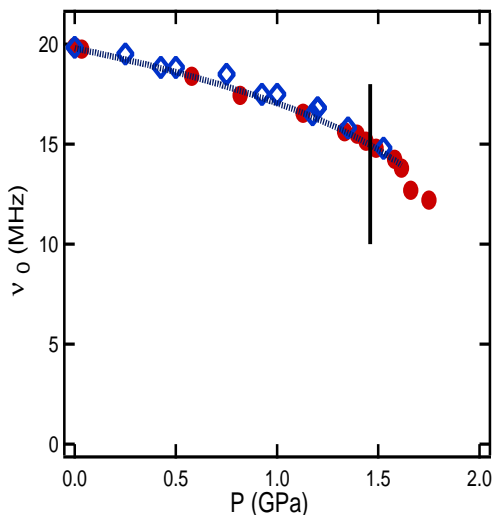


FIG. 1: Resonant frequency ν_0 of the NMR absorption at different pressures (solid circles). Dashed line is a guide to the eye. Diamonds represent the saturation magnetization data from Ref. [22].

transport behavior seen for pressures exceeding P^* can be attributed to the magnetic inhomogeneity. We make the important acknowledgment that there are conflicting reports in the literature regarding the existence of a magnetic phase for $P > P_c$ in MnSi [19]. In the results reported here, we have kept track of the mean pressure and assign an upper bound to the extent of pressure inhomogeneities. We accounted for the frequency dependence of our sensitivity and rf enhancement factors in normalizing the signal intensities.

The MnSi samples were made by a rf induction melting technique. The materials were ground to a grain size $d \approx 10 \mu\text{m}$ in order to achieve significant bulk rf penetration. At this size, we found rf enhancement factors are independent of rf power levels. The transverse spin relaxation T_2 was measured by the spin echo technique, while the longitudinal spin relaxation rate T_1^{-1} was measured by the inversion-recovery method, with proper phase cycling to remove any stimulated echoes from the accumulated transients. Perhaps because the ground state is a helimagnet, no evidence for domain wall contribution was found in the powdered samples as one might find for ferromagnets [20]. The applied pressure at low temperature was calibrated by measuring the ^{63}Cu NQR frequencies in Cu_2O powder [21] mixed with the MnSi and placed in the same coil. The mean pressure could be established to within 0.01 GPa, and an upper bound for the pressure inhomogeneities was inferred from the linewidth of the ^{63}Cu NQR signal.

The resonant frequency vs. pressure recorded at $T = 1.8\text{K}$ is shown in Fig. 1. The values are taken to be the frequency of maximum NMR signal, $\nu_0(P, T = 1.8\text{K})$ swept frequency; we will return to this point below, as

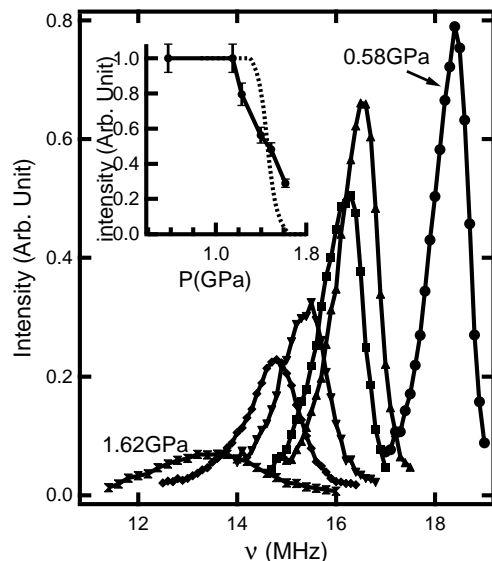


FIG. 2: Normalized ^{29}Si spectrum at six pressures, from right to left, $p = 0.58, 1.15, 1.23, 1.40, 1.49,$ and 1.62GPa . Inset: Comparison of total spectral intensity (solid circles) and the expected one (dashed line) due to pressure inhomogeneity, assuming a first order phase transition at $P_c = 1.46\text{GPa}$.

it relates to the pressure inhomogeneity. Our measurements at low temperatures show that ν_0 almost saturates at this temperature, and the overall variation is quantitatively similar to previous reports [19]. With increasing pressure, ν_0 decreases slowly up to 1.46GPa . This pressure, as indicated by the vertical line in the figure, is the critical pressure P_c where ac susceptibility measurements indicate $T_c \rightarrow 0$ [3]. Surprisingly, an NMR signal is still observed up to 1.75GPa , accompanied by a fast drop of resonance frequency and intensity. Although the spectrum is further inhomogeneously broadened with increasing pressure, the peak feature remains well-defined to highest pressures.

Before presenting the relaxation rates, we would first like to address the experimental significance of the high-pressure NMR signal. As there is no applied field, its presence indicates local static magnetism, on NMR time scales, for $P > P_c$. While it is compelling to attribute this observation to pressure inhomogeneities, the linewidths of the ^{63}Cu NQR signal are too narrow to support that interpretation. An indication that our results for the pressure dependence of the static moments are consistent with independent measurements comes from a comparison of the bulk saturation moments [22] and ν_0 over a range of pressures. The two results are shown in Fig. 1; the moments are normalized to the NMR frequencies using *only* A_{hf} .

The ^{29}Si spectrum at different frequencies are scaled to correct for temperature- and frequency-dependent sensitivities, as well as for the rf enhancement of the magnetic phase. Figure 2 shows the normalized intensity at

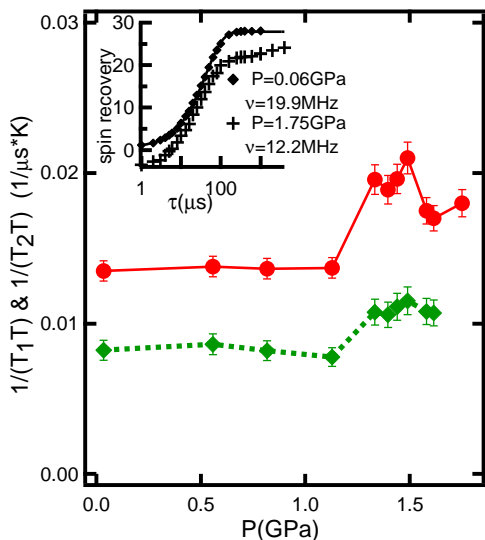


FIG. 3: Spin-lattice relaxation rate $T_1^{-1}(\nu_0)$ (circles) and spin-spin relaxation rate $T_2^{-1}(\nu_0)$ (diamonds) at different pressures. In the inset is a comparison of longitudinal magnetization recovery for a pressure $P < P^*$, and $P = 1.75 \text{ GPa}$. The amplitudes of the recoveries are adjusted for clarity, and the solid line is a single-exponential recovery.

six different pressures. In addition to the decrease of the central resonance frequency ν_0 with pressure, the spectra are inhomogeneously broadened at all pressures. Sample and pressure inhomogeneities both contribute to the line broadening. The pressure inhomogeneity that occurs in the solidified pressure medium (Flourinert Fc-75) is determined from the temperature-dependent linewidth of ^{63}Cu NQR spectrum. At $T = 1.8 \text{ K}$, the spectrum is near to Lorentzian shape, and the resulting pressure inhomogeneity gives $\Delta P/P \approx 4\%$, that is, $\Delta P \approx 0.06 \text{ GPa}$ at $P = 1.5 \text{ GPa}$. In addition, the ^{29}Si spectrum at $P = 0.58 \text{ GPa}$ is noticeably asymmetric, with the weight of the low frequency tail larger than the high frequency side. This indicates the phase is inhomogeneous, although we are not sure if this is intrinsic or due to quenched disorder. The integrated spectral intensity at different pressures are plotted in the inset of fig. 2. An unexpected intensity loss is seen from 1.2 GPa , which is labeled as P^* . For comparison, the expected spectrum due to pressure inhomogeneity, assuming a first order phase transition at $P_c = 1.46 \text{ GPa}$, is also plotted in the inset of Fig. 2. The range of pressures over which we observe the decrease of the signal is much wider than we would predict from the upper bound on the pressure variation alone.

The relaxation rates, for longitudinal and transverse relaxation, are plotted as a function of pressure in Fig. 3. For fixed pressure, transverse spin relaxation follows the relation $\nu_0^2/T_1T = \text{constant}$ at low temperatures, as expected from spin fluctuation theory [23] and previously observed [14, 19]. However, For pressures below P^* ,

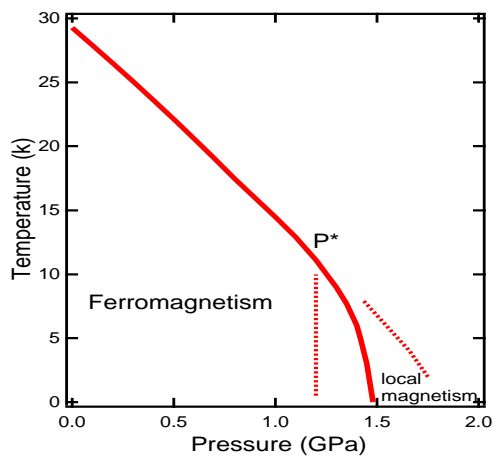


FIG. 4: A phase diagram after [3] (solid line) and an onset of inhomogeneous phase between dotted lines from present NMR measurements.

$1/T_1T$ is independent of pressure even though ν_0 dropped by 25%. We also observed that T_2 is proportional to T_1 , with $T_2/T_1 \approx 5/3$. Assuming that the spin-lattice relaxation is dominated by fluctuations in the hyperfine field, we expect that $T_2 = T_1$ when the same fluctuations dominate the spin echo decay and they are isotropic. The anisotropy of the ordered phase leads to much larger field fluctuations in the direction transverse to the average spin orientation, and the unusual result $T_2 > T_1$ [24]. Above P^* , however, both $1/T_1T$ and $1/T_2T$ increases dramatically and peaks near to P_c . This observation, together with the signal loss for $P > P^*$, suggests that the high-pressure phase has different properties from the long-range ordered helical phase observed at lower pressures. In addition, the longitudinal spin recovery for both below and above P^* are adjusted and compared in the inset of Fig. 3. In contrast to the behavior at low pressures $P < P^*$ where the recovery is always described by a single exponential, the non-exponential recovery observed when $P > P^*$ demonstrates that there are quite different environments and further work is necessary to clarify the details.

For comparison, the ferromagnet transition temperature after Ref. [3] is plotted as the solid line in Fig. 4. From present NMR measurements, we propose inserting another: The nearly vertical line at P^* is our estimate for the onset of phase inhomogeneity. The other is merely demarking the range of temperature and pressure where local magnetism was detected. That is, where sites with static moment $\mu \geq 0.2\mu_B$. Due to the reduction of the signal intensity and tank circuit sensitivity, it became impractical to quantify the signal strength below $\approx 10 \text{ MHz}$, although there is no reason to suspect that there are not ^{29}Si nuclei with correspondingly low Larmor frequencies, particularly at higher pressures.

It is compelling to cast these results in the context of a

model recently advanced to explain high-pressure resistivity measurements on very clean, single crystal MnSi [9, 17]. In zero applied magnetic field, the principle observation is that to the lowest measured temperatures, the temperature-dependent part of the resistivity $\Delta\rho \cong T^2$ for $P < P_c$, and $\Delta\rho \cong T^{3/2}$ for $P > P_c$. Remarkably, the non-Fermi Liquid exponent persists at least to the maximum reported pressure tested, namely $P = 2.75\text{GPa}$. The authors propose that droplet-like phase inhomogeneity occurs as a result of proximity to the tricritical point. Under some conditions, such a model would lead an NMR signal as observed. However, the inhomogeneities observed in the ^{29}Si NMR signals over such a wide range of pressures about P_c could also point to the importance of static disorder in the vicinity of the quantum phase transition. On the other hand, non-magnetic quenched disorder is expected to suppress the first order transition and inhomogeneities that result [25]. Perhaps competing interactions are relevant here, as they are known to be important in MnSi: for example, $\text{Mn}_9\text{Rh}_1\text{Si}$ is a spin glass [26]. Further exploration of dynamics associated with the NMR signals, in principle, could give further justification to models based on fluctuations of P_c in clean systems.

To summarize, ^{29}Si NMR spectroscopy and dynamics in MnSi under pressure demonstrate the existence of static magnetism persisting to higher pressures than previously recognized. In particular, we observe a zero-field ^{29}Si NMR signal at 1.75GPa even though the cited critical pressure is $P_c \approx 1.46\text{GPa}$. We calibrated the pressure using the ^{63}Cu NQR line in Cu_2O , and used it to rule out pressure variations as the reason for our observations. There is a large pressure dependence to the signal intensity starting from $P^* = 1.2\text{GPa}$. It may be fortuitous, but this is precisely the pressure where the magnetic ordering transition changes from second order to first order. The change in the spin dynamics, which we infer from the larger value of $(T_1T)^{-1}$ indicates that the inhomogeneous magnetism is locally different from the helimagnet at low pressures. NMR experiments in a magnetic field could be used to determine whether the higher pressure magnetism remains helical. Although we are unaware how much disorder plays a role in this phase, the unexpected properties observed in this class of itinerant ferromagnet near P_C can be related to this inhomogeneity. A droplet model proposed by Doiron-Leyraud, *et al.* [17], could lead to an NMR signal with a dynamic signature that can be observed.

ACKNOWLEDGMENTS

The work performed at UCLA and FSU was supported by the National Science Foundation under grant numbers DMR-0203806 (SB) and DMR-0203214 (ZF). Work at Los Alamos National Laboratory was performed under

the auspices of the U.S. Department of Energy. The authors were benefited from discussions with W.G. Clark, S. Kivelson, W. Hines, and J. Budnick.

-
- [1] J. A. Hertz, Phys. Rev. B **14**, 1165 (1976); A. J. Millis, Phys. Rev. B **48**, 7183 (1993).
 - [2] J. D. Thompson, Z. Fisk, and G. G. Lonzarich, Physica B **161**, 317 (1989).
 - [3] C. Pfleiderer, G. J. McMullan, S. R. Julian, and G. G. Lonzarich, Phys. Rev. B **55**, 8330 (1997).
 - [4] Pfleiderer, *et al.*, Nature **412**, 58 (2001)
 - [5] S. S. Saxena, *et al.*, Nature **406**, 587 (2000)
 - [6] N. D. Mathur, *et al.*, Nature **394**, 39 (1998).
 - [7] V. A. Sidorov *et al.*, Phys. Rev. Lett. **89**, 157004 (2002).
 - [8] P. Coleman, Physica B **259-261**, 353 (1999).
 - [9] C. Pfleiderer, S. R. Julian, and G. G. Lonzarich, Nature **414**, 427 (2001);
 - [10] T. Moriya, *Spin Fluctuations in Itinerant Electron Magnetism* (Springer, Berlin, 1985) and references therein.
 - [11] H. J. Williams, J. H. Wernick, R. C. Sherwood, and G. K. Worthier, J. Appl. Phys. **37**, 1256 (1966); D. Bloch, J. Voiron, V. Jaccarino, and J. H. Wernick, Phys. Lett. **51A**, 259 (1975).
 - [12] Y. Ishikawa, G. Shirane, J. A. Tarvin, and M. Kohgi, Phys. Rev. B **16**, 4956 (1977); Y. Ishikawa, Y. Noda, C. Fincher and G. Shirane *et al.*, Phys. Rev. B **25**, 254 (1982).
 - [13] H. Yasuoka, V. Jaccarino, R. C. Sherwood, and J. H. Wernick, J. Phys. Soc. Jpn. **44**, 842 (1978).
 - [14] R. Kadono *et al.*, Phys. Rev. B **42**, 6515 (1990); R. Kadono *et al.*, Phys. Rev. B **48**, 16803 (1993); I. M. Gatmalureanu *et al.*, Phys. Rev. Lett. **90**, 157201 (2003).
 - [15] Y. Ishikawa, K. Tajima, D. Bloch, and M. Roth, Solid State Commun. **19**, 525 (1976).
 - [16] O. Nakanishi, A. Yanase, A. Hasegawa, and M. Kataoka, Solid State Commun. **35**, 995 (1980); P. Bak and M. H. Jensen, J. Phys. C: Solid State Physics **13**, L881 (1980).
 - [17] N. Doiron-Leyraud *et al.*, Nature **425**, 595 (2003).
 - [18] K. Motoya, H. Yasuoka, Y. Nakamura, V. Jaccarino, and J. H. Wernick, J. Phys. Soc. Jpn. **44**, 833 (1978).
 - [19] C. Thessieu, K. Ishida, Y. Kitaoka, K. Asayama, and G. Lapertot, J. Magnetism and Magnetic Materials, **177-181**, 609 (1998); C. Thessieu, Y. Kitaoka, K. Asayama, Physica B **259-261**, 847 (1999).
 - [20] M. Weger, Phys. Rev. **128**, 1505 (1962).
 - [21] A. P. Reyes, E. T. Ahrens, R. H. Heffner, P. C. Hammel, and J. D. Thompson, Rev. Sci. Instrum. **63**, 3120 (1995).
 - [22] K. Koyama, T. Goto, T. Kanomata, and R. Note, Phys. Rev. B **62**, 986 (2000).
 - [23] T. Moriya and K. Ueda, Solid. State. Commun. **15**, 169 (1974).
 - [24] see, *e. g.*, C. P. Slichter, *Principals of Magnetic Resonance*, Springer, 1990.
 - [25] D. Belitz, T. R. Kirkpatrick, and T. Vojta, Phys. Rev. Lett. **82**, 4707 (1999).
 - [26] W. Yu, J. D. Thompson, J. L. Sarrao, E. D. Bauer, M. E. Torelli, Z. Fisk, F. Zamborszky and S. E. Brown, unpublished.